

Ab initio comparative study of structural and electronic properties of mono- and multi-layer graphene and graphitic ZnO

N. KOUAYDI, M. KADDES, M. ZEMZEMI*

Laboratory of Physics of Materials and Nanomaterials applied to Environment, Faculty of Sciences of Gabes, University of Gabes, Erriadh City, Zrig, 6072 Gabes, Tunisia

Structural and electronic properties of the zinc oxide and the carbon were investigated using first-principle approaches. This work aims to follow the relative stability between wurtzite and graphitic structures of ZnO at a thickness of four layers. Our results prove that the graphitic structure becomes more stable. To validate our study in the passage between mono and multilayer in graphitic ZnO, we have conducting a parallel study on graphene and graphite. The ZnO structures are found to be semiconductor with a direct band gap. The energy band gap increase from wurtzite to graphitic structure by increasing the number of layers.

(Received September 24, 2020; accepted October 7, 2021)

Keywords: Graphitic ZnO; ZnO monolayer, Graphene; graphitic structure, Density functional theory (DFT), Electronic properties

1. Introduction

The potential of nanoscale has always provoked scientific discussions, and recent attempts to develop generally accepted design, growth and characterization procedures for this scale are underway. Dimensionality is one of the most fundamental material parameters, which not only defines the atomic structure of the material, but also determines its properties to a significant degree. The same compound can exhibit different properties in different dimensions [1]. A novel class of low-dimensional systems distinguishes the development of nanoscale sciences. One-dimension (1D) and two-dimension (2D) like nanowires, nanosheets, nanofilms and nanotubes have been one of the interesting subjects due to their remarkable properties and potential applications in a wide range of fields [2, 3]. Two-dimensional materials have attracted tremendous attention due to their unique nature that not only enriches the world of low-dimensional physics, but also provides a unique platform for transformative technical innovations [4, 5, 6]. The discovery of a whole family of 2D materials and their novel properties represents a fundamental and applied challenge Graphene has a prestigious position as future material for nanoelectronics and mechanics. Materials like hexagonal-boron nitride (h-BN) [7] and transition-metal dichalcogenides (MoS₂) [8] are also of great interest in the world of 2D materials. More recently, based on first-principles calculations, it was predicted that Si and Ge [9], even binary compounds of Group IV elements and III-V compounds [10] can form 2D stable monolayer honeycomb structures. Inspired by the extraordinary properties of graphene, researchers are exploring materials that have graphene-like structure. Graphene-like wurtzite

structure is adopted by binary II-VI and III-V compounds. Metal oxides are considered as favorite candidates for transparent conducting oxides (TCO). Zinc oxide (ZnO) have been widely studied thanks to its unique properties [11, 12, 13] ZnO which is an n-type semiconductor belongs to the family of transparent conductive oxides and has exceptional properties. In fact, it is characterized by a direct wide band gap (~ 3.37 eV) [14] at room temperature and a large exciton binding energy (~ 60 meV), which is the strongest value among all semiconductor compounds (GaN~25 meV, ZnS~20meV) [15], so it is a promising candidate material for optoelectronic and photovoltaic applications. It is non-toxic and abundant on the earth. ZnO is also considered as one of the rare multifunctional materials; its properties make it largely produced and used in a field of applications such as piezoelectric transducers, gas sensors, photocatalysis, light-emitting diodes (LEDs), laser diodes, the transparent electrodes (solar cells), as well as in the medical domain (blocking of UV dermatological creams), varistors, etc. [16-21]. ZnO exists in many crystallographic forms; wurtzite (P6₃mc space group), zincblende (F-43m) and rocksalt (Fm-3m). At ambient conditions, the wurtzite structure is the most stable. However, many studies proved that, at the nanoscale, this structure can be transformed into a new structure called graphite (only for few layers) [22]. Recently, it was found from Density Functional Theory (DFT) calculations that for ultra-thin films of ZnO, the graphite-like structure was energetically more favorable as compared to the wurtzite structure [23]. The graphitic ZnO (g-ZnO) is similar to the carbon graphite; Zn atoms and O atoms are located in the same plane. It is a honeycomb structure with space group P6₃/mmc (n° 194). The stability of this phase transformation from the wurtzite

lattice to a/the graphite-like structure is only limited to a thickness of few Zn-O layers and was subsequently verified by experiments [24]. A similar phase transition was also observed in the ZnO nanowire when it was subjected to uniaxial tensile loading [25]. The graphitic ZnO thin films are structurally similar to the multilayer of graphite and are expected to have interesting mechanical and electronic properties for potential nanoscale applications. It was studied by several authors. In fact, many theoretical works have proved the existence of graphite structure [26]. For example, Freeman *et al.* [22] and Zhang *et al.* [27, 28] have demonstrated that the wurtzite structure can be transformed into the graphite structure, but only for a few layers, defining a critical thickness. Moreover, Wu *et al.* [29] confirmed the previous result and found that the transition to be graphite structure only occurs below 3 layers. Until now, few experimental results have been reported in literature. In 2007, Tusche *et al.* [24] reported the graphite structure of ZnO found that the stability of this structure is limited to a thicknesses of a few atomic layers (the number is to be 3 or 4 layers).

In this work, to get a better understanding of the new structure of graphitic ZnO at the nanoscale, we have investigated their structural and electronic properties using *ab initio* calculations based on density functional theory. We discuss the relative stability between graphitic and wurtzite phases of ZnO at a thickness of four layers. We also study the effect of the wurtzite-graphite structure change on the electronic properties. To interpret our results, we have presented the properties of graphene and graphite as reference materials in the field of mono- and multilayer.

2. Computational methods

First-principles calculations of structural and electronic properties of zinc oxide have been performed in the framework of the Density Functional Theory [30], using pseudopotentials and a plane wave basis set as implemented in the Abinit code [31]. For the plane wave basis set, the energy cutoff is set to be 50 Hartree. Troullier-Martins pseudopotentials [32] have been generated by means of the Fritz-Haber-Institute package [33], for the reference $3d^{10}4s^2$ and $2s^22p^4$ atomic configurations of zinc and oxygen, respectively. The suitable atomic configuration of carbon in graphite and graphene is $2s^22p^2$. We select the local density approximation (LDA) and the generalized gradient approximation (GGA) as the exchange and correlation potential for our work. The parameterization in LDA is that of Perdew and Wang [34], which is based on the quantum Monte Carlo calculations of Ceperley and Alder [35]. In search of a better approximation to describe the exchange-correlation density functional, we also use the Perdew-Burke-Ernzerhof (PBE) version of the generalized gradient approximation [36]. The k-point samplings with $8 \times 8 \times 8$ for bulk and $8 \times 8 \times 1$ for monolayer structures have been used after convergence test in the Brillouin zone

using the Monkhorst-Pack scheme [37]. We adopted a supercell technique for modeling the mono- and multilayer structures. To avoid the interactions of adjacent slabs, the vacuum space of 15 \AA is used included along the Z direction. All the geometric structures in this article are plotted using XCrySDen software [38].

3. Results and discussion

3.1. Structural properties

3.1.1. Multilayer structure

Zinc oxide is an II-VI compound semiconductor, where most of the compounds of this family crystallize in the wurtzite structure.

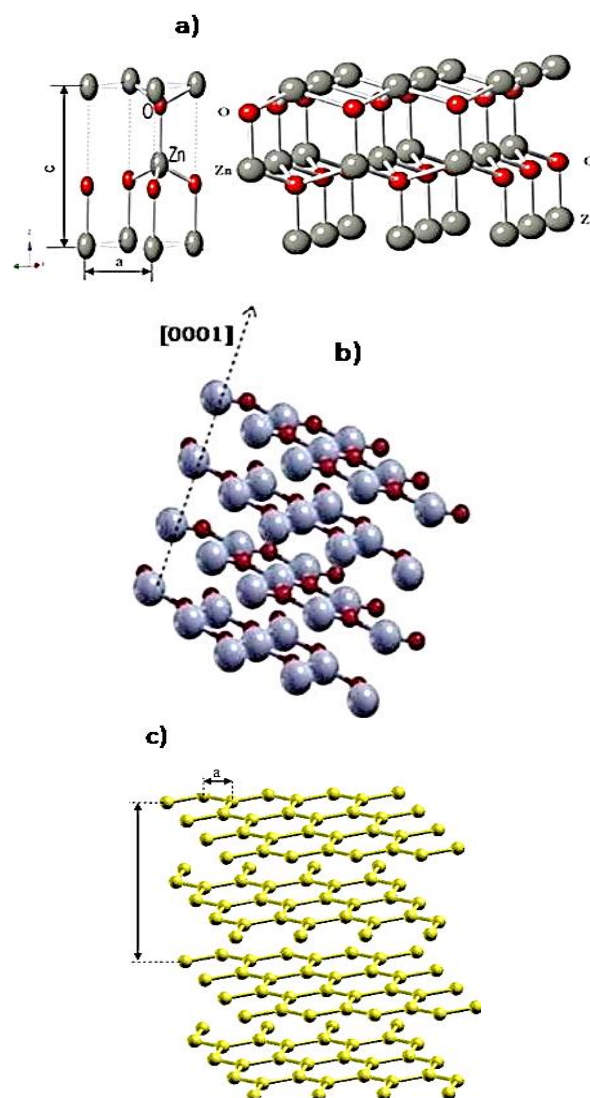


Fig. 1. Schematic representations of the crystal structures of ZnO (a) wurtzite, (b) graphitic ZnO and (c) graphite (color online)

Wurtzite structure has a hexagonal unit cell with two lattice parameters (a , c) and belongs to the space group

P6₃mc (No. 186). Under ambient conditions, ZnO crystallizes in the wurtzite structure. This structure is characterized by two interconnected sublattices of Zn²⁺ and O²⁻ in such a way that Zn ion is surrounded by a tetrahedral of O ions, and vice-versa (Fig. 1 (a)). Under high pressure, the wurtzite phase transforms into a cubic rocksalt or zincblende. These phase transitions were studied both theoretically and experimentally [39].

The first step of this study will be the analysis of the structural properties; the equilibrium lattice parameters are calculated within the method seen previously using the habitual minimization procedure [40]. The total energy was calculated for different values of the lattice constant, and the ground state corresponds to the lowest value of the total energy. A fit of the resulting energy versus volume curve with the Murnaghan equation [41], shown in Fig. 2, gives the values of the equilibrium lattice parameters for

the different polymorphs of ZnO. We show in Fig. 2 that the wurtzite phase is lower in energy than the others phases which proves the more stability of the wurtzite structure. Our calculated lattice parameters were recorded and compared with values obtained from other simulations and experiments as summarized in Table 1. Our calculations are based on the local density approximation (LDA) and generalized gradient approximation (GGA-PBE). It was observed that the deviation of the lattice parameters is less than 1% of the experimental values, which may be due to the approximation method used during optimization. LDA calculations show the well-known over-binding effect value with a lattice parameter underestimated as compared to the experimental results, and GGA-PBE calculations are overestimated. Our results are in a good agreement with the published experimental and theoretical data.

Table 1. The optimized lattice parameters of ZnO in different structures and graphite

Structure		Present work		Exp.	Other calculations
		LDA	GGA		
ZnO (Wurtzite)	a	3.21	3.32	3.24 [42]	3.192 [43] 3.209 [44]
	c	5.22	5.29	5.20 [42]	5.190 [43] 5.128 [44]
ZnO (Zincblende)	a	4.53	4.66	4.46 [45]	4.505 [44]
ZnO (Rocksalt)	a	4.24	4.36	4.28 [42]	4.224 [44] 4.339 [46]
ZnO (graphitic)	a	3.23	3.31	3.44 [47]	3.161 [44] 3.397 [48]
	c	5.87	6.93	-	5.294 [44] 5.132 [48]
Graphite	a	2.43	2.48	2.45 [49]	2.458 [50] 2.597 [51]
	c	6.20	7.09	6.69 [49]	6.674 [50] 7.080 [51]

We considered 3D bulk ZnO, which is in wurtzite, zincblende and rocksalt. However, it was found from Density Functional Theory calculations that for ultra-thin films of ZnO, the graphite-like structure (g-ZnO) was energetically more favorable as compared to the wurtzite structure [23]. The g-ZnO structure consists of ABAB... stacking sequence along the [0001] direction and Zn atoms and O atoms are located in the same plane (Fig. 1 (b)). This structure belongs to the space group P6₃/mmc (No. 194). Atoms in wurtzite and zincblende structures are four fold coordinated through tetrahedrally directed sp³

orbitals, whereas the atoms in the g-ZnO crystal are three fold coordinated through sp² orbitals. Among the goals of this work is to study and compare the stability of the g-ZnO and the other 3D structures (wurtzite, zincblende, rocksalt). To accomplish this goal, we always use energy versus volume. Fig. 2 shows the total energy as a function of volume for ZnO in the 3D bulk structures. These curves clearly show that for all compounds, the wurtzite form is slightly lower in energy. g-ZnO is higher in energy, confirming that this form is less stable. It is worth noticing that results from both LDA and GGA are the same.

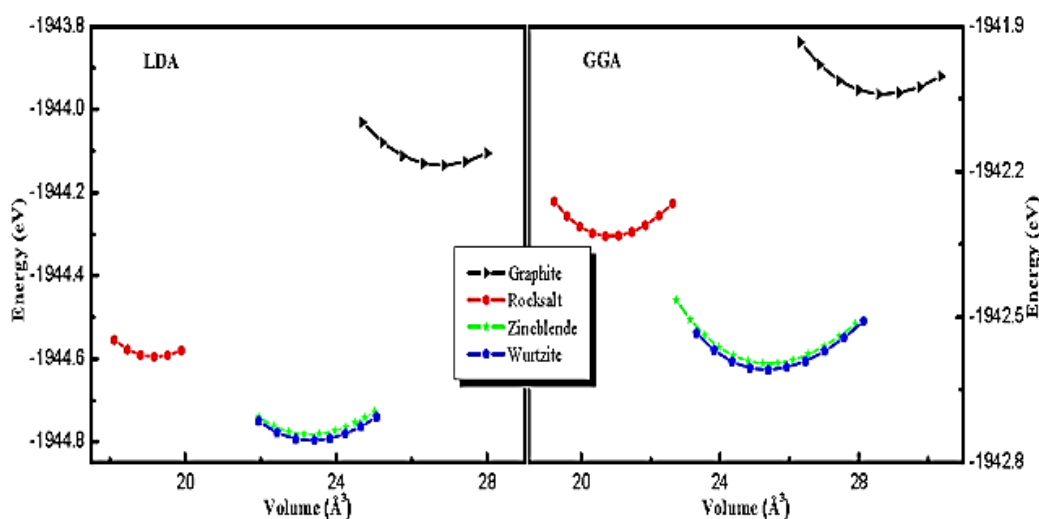


Fig. 2. Variations of the ZnO total energy as a function of the volume, for 4 phases, Wurtzite, Zincblende, Rocksalt and Graphite within LDA and GGA approximations (color online)

The structural parameters for the different phases of ZnO are determined. The results and comparison to experiment and other theoretical works are summarized in Table 1. Our results are in good agreement with others studies [42- 48]. To understand the properties of g-ZnO we studied the graphite. Graphite is the most stable form of carbon under standard conditions. The carbon atoms are arranged in a honeycomb structure. The coordinates of the atoms on the same plane are $(0, 0, 0)$ and $(1/3, 2/3, 0)$. The atomic planes are spaced by distance c (Fig. 1 (c)). Graphite belongs to the space group $P6_3/mmc$. By adopting the same work strategy that is based on the variation of energy according to the lattice parameter, we calculated the equilibrium lattice parameters of graphite. Table 1 summarized the equilibrium lattice parameters of

graphite with other parameters available in the literature. These results are in a good agreement with experimental data and other first-principles calculations [49-51]. To reveal the dimensionality effects, our study includes also 3D bulk ZnO (wurtzite, zincblende, rocksalt, graphite) and a new structure that appears for some atomic layers of thickness. It was observed that 3D bulk ZnO transforms to 2D stable honeycomb structures [25]. The stability of this phase transformation from 3D ZnO lattice to 2D ZnO film is only limited to a thickness of several ZnO layers and was subsequently verified by experiment [24]. The standard procedure for calculating total energy is the slab supercell technique. In this work, we modeled a slab of ZnO in the honeycomb structure with a supercell employing 4 layers (Fig. 3).

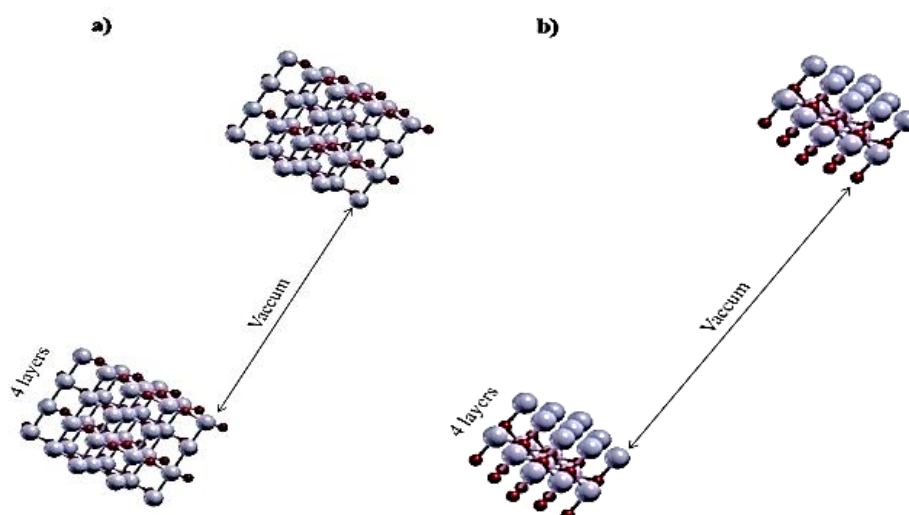


Fig. 3. Supercells representing the (a) four layers of graphitic ZnO and (b) four layers of wurtzite ZnO (color online)

In this study, we considered two configurations following the crystalline structure. The first structure is wurtzite (Fig. 3 (a)) where alternating zinc and oxygen layers occur. The second is a graphite structure (Fig. 3 (b))

where the zinc and oxygen atoms are on the same plane. The vacuum region of the $3c$ -parameter ($\sim 15\text{\AA}$) ensures the decoupling of repeated slabs. Exploiting the curves of energy as a function of volume for these two structures,

we can observe clearly from Fig. 4 that the graphite structure is energetically lower than the wurtzite structure. So, it appears that the graphite structure is the most stable structure. This result is confirmed by many previous results [22, 24, 29]. Our calculations are verified by the LDA and GGA approximations. The lattice parameters a and c were optimized by calculating the total energy as a

function of volume and fitting the curves with the Murnaghan equation of state. In this case, the lattice constant a (i.e. the interatomic distance) is reduced by $\sim 3\%$ and the interlayers distance c is increased by $\sim 20\%$. Our results are in good agreement with the values available in literature.

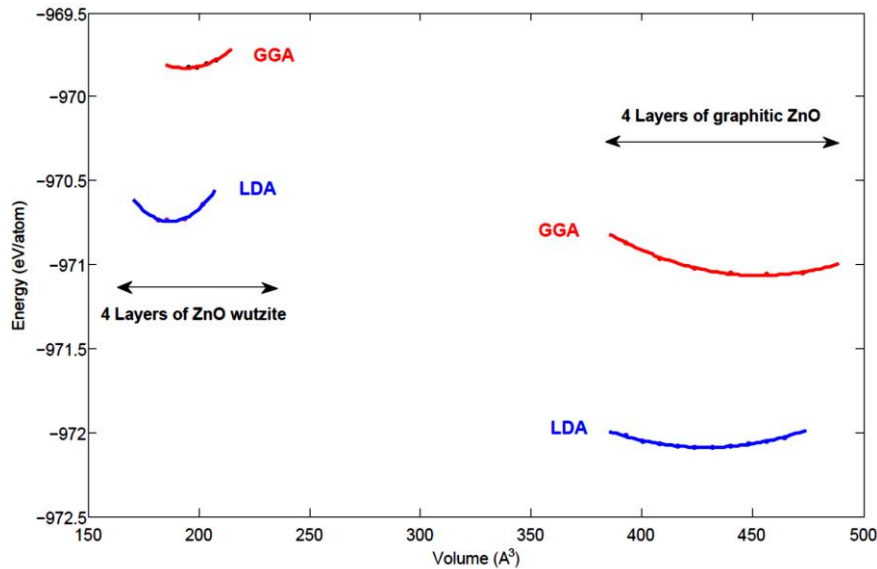


Fig. 4. Total energy as a function of the volume for 4-layers ZnO; wurtzite and graphite with the LDA and GGA approximations (color online)

3.1.2. Monolayer structure

A good understanding of the novel properties of two-dimensional semiconductors requires a good understanding of the structural properties. In this study, we focused on the monolayer structural properties of graphene and ZnO monolayer. Monolayer structure consists of atoms arranged with a two-dimensional honeycomb crystal structure as shown in Fig. 5 (a). The honeycomb structure consists of the hexagonal Bravais lattice, with a basis of two atoms, at each lattice point we associate the primitive lattice vectors of the hexagonal Bravais lattice, $\vec{a}_1 = \sqrt{\frac{3}{2}}\vec{x} + \frac{3}{2}\vec{y}$ and $\vec{a}_2 = -\sqrt{\frac{3}{2}}\vec{x} + \frac{3}{2}\vec{y}$ (Fig. 5 (a)). The lattice constant is the distance between carbon atoms in the graphene and between oxygen and zinc in the zinc oxide monolayer. Fig. 5 (b, c) shows a structure of graphene and ZnO monolayer. The variation of energy according to the lattice parameters allows us to calculate the equilibrium lattice parameters of graphene and ZnO monolayer.

Table 2. The optimized lattice parameters of ZnO monolayer and graphene

Structure	a (Å)	References	
		LDA	Present work
ZnO monolayer	3.228	LDA	Present work
	3.313	GGA	
	3.290 [52]	Other calculations	
	3.232 [53]		
3.303 [24]	Experiment		
Graphene	2.433	LDA	Present work
	2.457	GGA	
	2.461 [54]	Other calculations	
	2.445 [55]		
	2.454 [56]	Experiment	

The calculations based on DFT-LDA approximation usually exhibit under estimation values as compared to experimental data, while the calculations based on DFT-GGA approximation overestimates it. Ours results and other theoretical and experimental results are listed in Table 2 [24, 52-56].

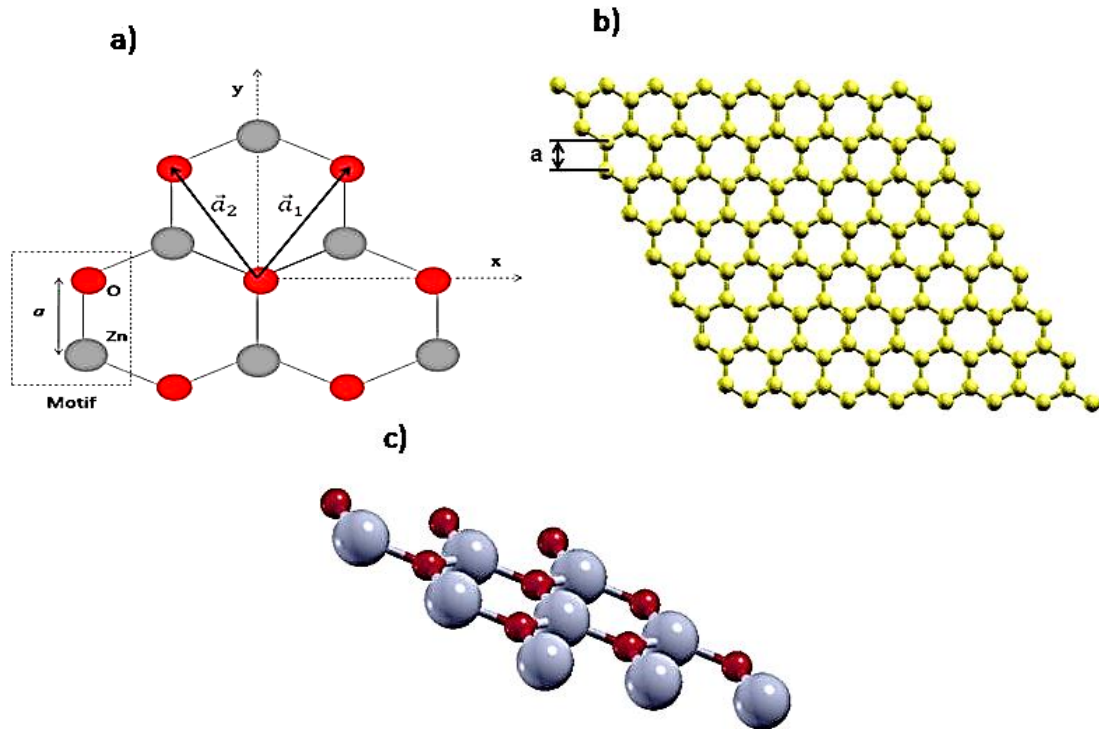


Fig. 5. Atomic structure of (a) Schematic representation of a ZnO layer, \vec{a}_1 and \vec{a}_2 are the basis vectors of the hexagonal Bravais lattice, (b) graphene and (c) ZnO monolayer (color online)

3.2. Electronic properties

3.2.1. Multilayer structure

In this part, we are interested in the electronic properties of ZnO in wurtzite, g-ZnO structure and g-ZnO four layers slab, and we perform an analysis of the electronic band structure of these crystalline phases. The energy band structures of ZnO in its different phases have been calculated and plotted along the high symmetry directions in the Brillouin zone K- Γ -M-K, as shown in Fig.

6 (a), (b) and (c). The Fermi level (E_F) is fixed at 0 eV. For all these structures, the valence band maximum is found to be 0 eV at Γ point. The band structure has been evaluated using the local density approximation (LDA). The wurtzite ZnO (Fig. 6(a)) shows a direct band gap of 0.763 eV which is in excellent agreement with other theoretical values (0.77 eV [57] and 0.81 eV [58]). It is smaller than that of the experimental result; $E_g = 3.37$ eV [14]. This is a confirmation that the theoretical band gaps are underestimated within LDA in comparison with the experimental values.

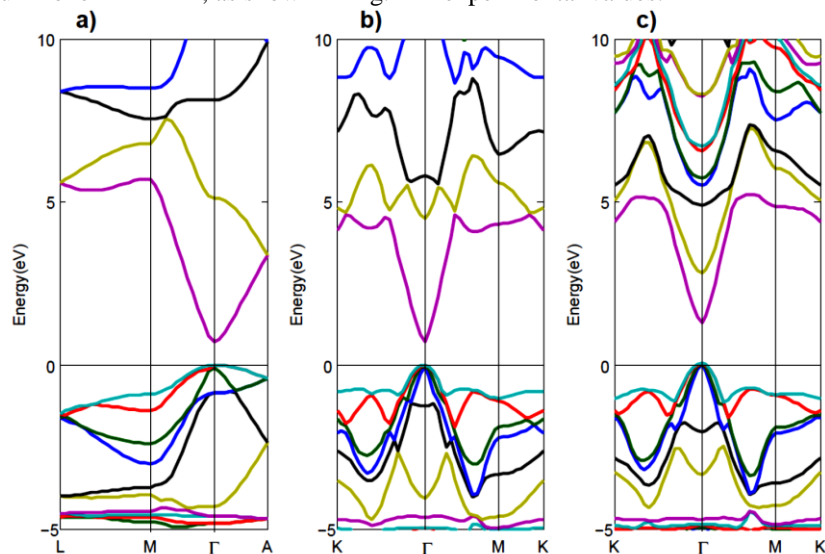


Fig. 6. Band structures of ZnO along the principle high symmetry directions in the first Brillouin zone for (a) wurtzite, (b) g-ZnO bulk and (c) g-ZnO four layers (color online)

We also analyse the band gap structure of the g-ZnO bulk structure and the g-ZnO four layers slab. These two structures, presented in Fig. 6 (b) and (c), have also a direct band gap. Until now, no experimental results have been reported about the electronic properties of the g-ZnO structure. Consequently, most works of literature reported are theoretical researches. We have obtained $E_g = 0.717\text{ eV}$ for g-ZnO structure. This result is in good agreement with the results of Su *et al.* ($E_g = 0.838\text{ eV}$ under the hydrostatic pressure) [59] and Kang *et al.* ($E_g = 0.967\text{ eV}$) [47]. Our calculation of the band gap of the ZnO four layer slab is $E_g = 1.76\text{ eV}$. Our results are in good agreement with these previous calculations. The g-ZnO four layers slab has an energy band gap larger than the wurtzite and g-ZnO bulk structure. About the band structure, it is well known that the local density approximation (LDA) underestimates the energy gap. Therefore, to correct this energy and to have an approximately exact value of E_g , many groups used the GGA+U, the HSE06 or the PBE0. Based on these approximations, the energy band gap of ZnO has been

predicted to be $3.89 - 5.30\text{ eV}$ by Zheng *et al.* [60] and 3.82 eV by Wang Q. B. *et al.* [48]. This difference between different values can be explained by the instability of the graphite phase, which may be regarded as a hypothetical phase until now. In Fig. 7, we illustrate the calculated density of states (DOS) for the three different forms of ZnO (wurtzite, g-ZnO and g-ZnO four layers). For these structures, our results show that the valence band (VB) state are composed mainly of O-2s, O-2p and Zn-2s states while the conduction band (CB) is dominated by/ comes mainly from the Zn-4s states [61, 62].

The DOS values of ZnO wurtzite and g-ZnO are similar. But, the four layers of g-ZnO showed a more intense peak in the DOS at the Fermi level. This property is a sign of instability, according to Hume-Rothery [63]. The increase in the number of layers increases the quantity of energy level, which raises the density of states (DOS). Therefore, the consequence is that the valence band energy becomes higher than the Fermi level. Consequently, the gap energy decreases with the increase in the number of layers (Fig. 6).

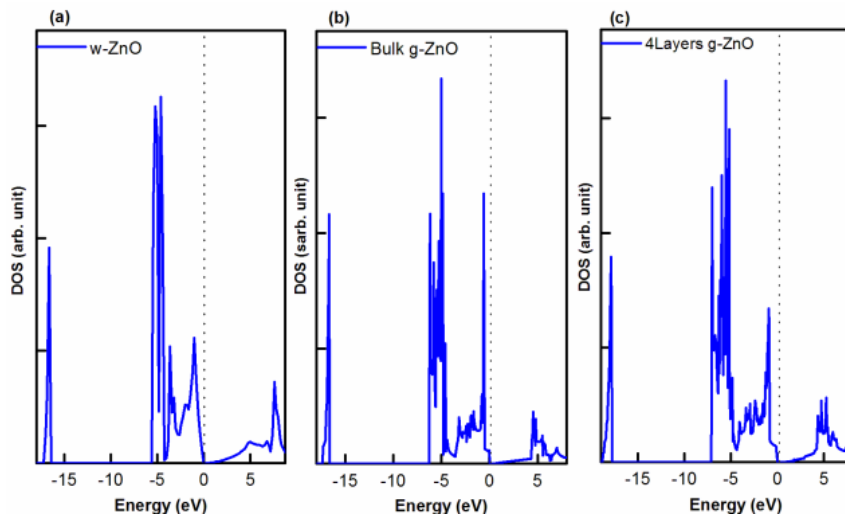


Fig. 7. Density of states (DOS) of ZnO in the three forms, (a) wurtzite, (b) g-ZnO bulk and (c) g-ZnO four layers (color online)

3.2.2. Monolayer structure

The electronic properties of the ZnO monolayer allow us to draw several conclusions about the nature of this form of zinc oxide. To calculate the band structure of the ZnO monolayer, we have chosen the direction of high symmetry in the first Brillouin zone K- Γ -M-K. Fig. 8-b illustrates the structure of monolayer zinc oxide with LDA approximation. This figure shows that the ZnO monolayer is a direct gap semiconductor at the point Γ . The energy values of the gap for the ZnO monolayer are 1.66 eV for LDA approximation and 1.69 eV for GGA approximation obtained by the pseudopotential approach (PP). This value is predicted to be 1.762 eV by Tu [64], 1.68 eV by Topsakal [57], 1.84 eV by Wang Y. *et al.* [65] and 1.67 eV [42, 52, 53, 66]. To better understand the electronic properties of monolayer structures, we calculate the band structure of graphene. Our calculation was carried out along the K- Γ -M-K path of high symmetry directions in

the first Brillouin zone. Fig. 8 (a) shows the electronic bands structure of graphene within LDA approximation. This figure does not show a band gap between the valence band and the conduction band. The two bands are connected at Fermi level is equal to 0 eV . This calculation clearly shows that graphene has a semi-metallic behavior (semiconductor with a zero band gap). This result is consistent with other theoretical and experimental studies [55, 67]. From bulk to monolayer structures, the band structures undergo changes that can change the character and the use of this material. The controllability of the band gap may also be used to optimize the materials used. With decreasing thickness, band structures of graphite pass from semiconductor to semi-metal (zero gaps). ZnO bulk and monolayer keep a direct gap but the value of the band-gap decrease. This specificity of the ZnO monolayer to have a band-gap different from zero can make this material more important than the graphene where its zero band-gap limits

its use in several fields where one seeks band-gap energy non-zero.

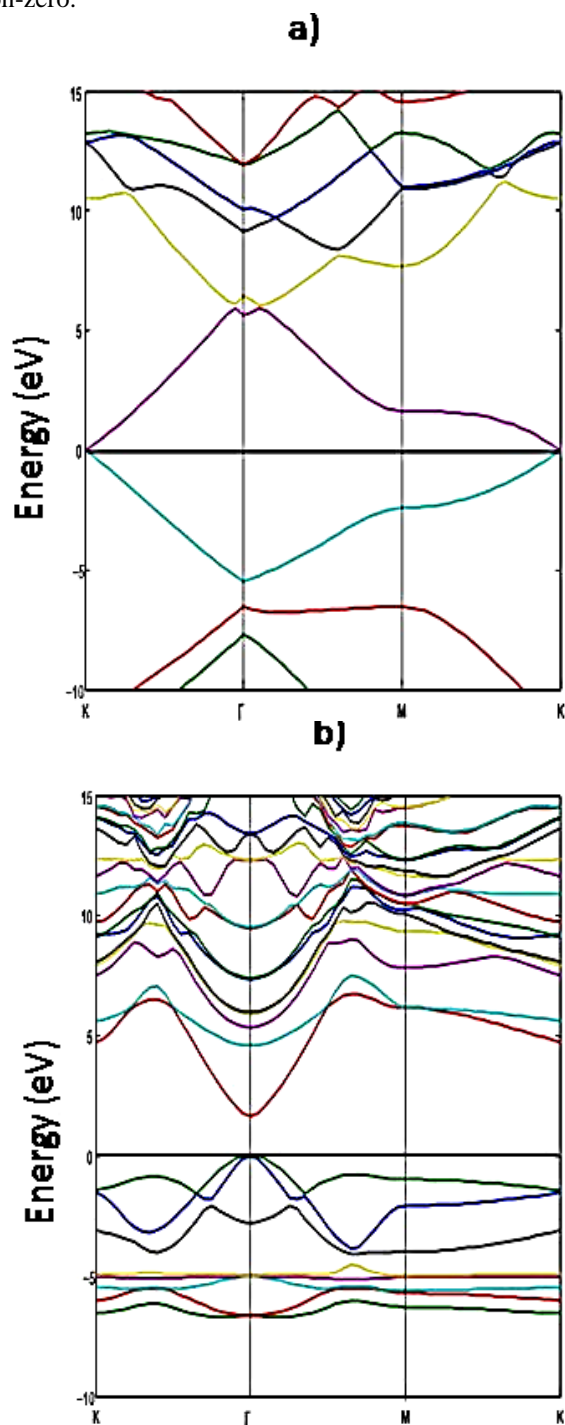


Fig. 8. Band structures of (a) graphene and (b) ZnO monolayer (color online)

4. Conclusion

In summary, the first-principle calculations are performed to investigate the structural and electronic properties of zinc oxide (monolayer, wurtzite and graphitic structures) and carbon (graphene and graphite structures). To discover the novel structure graphitic ZnO structure and its special and unique properties, we have studied the

relative stability between graphitic and wurtzite phases of ZnO at a thickness of 4 four layers. Unlike to the bulk, the graphite phase becomes more stable than the wurtzite structure of thin layers. This result is in excellent agreement with experimental data and other first-principles calculations. Similar to the previous theoretical reports, our results of electronic structure calculation show that the graphitic structure has a direct optical band gap of 1.76 eV. This result makes it a promising phase for technological nanoscale electronic and optoelectronic applications. We have also presented the properties of graphene and graphite as reference materials in the field of mono- and multilayer.

Acknowledgments

The authors wish to thank Professor S. Alaya for his helpful contributions to the present work.

References

- [1] A. Gupta, T. Sakthivel, S. Seal, *Prog. Mater. Sci.* **73**, 44 (2015).
- [2] N. H. Nickel, E. Terukov, *Zinc Oxide -A Material for Micro- and Optoelectronic Applications*, Springer, Netherlands, 2005.
- [3] M. Zemzemi, S. Alaya, *J. Optoelectron. Adv. M.* **16**(3-4), 471 (2014).
- [4] K. S. Novoselov, D. Jiang, F. Schedin, T. J. Booth, V. V. Khotkevich, S. V. Morozov, K. Geim, *Proc. Natl. Acad. Sci. U. S. A.*, **30**, 10451 (2005).
- [5] M. Debbichi, L. Debbichi, S. Lebègue, *Phys. Lett. A*, **384**, 126684 (2020).
- [6] M. Debbichi, L. Debbichi, S. Lebègue, *Phys. Lett. A* **383**, 2922 (2019).
- [7] D. Pacilé, J. C. Meyer, C. O. Girit, A. Zettl, *Appl. Phys. Lett.* **92**, 133107 (2008).
- [8] K. F. Mak, C. Lee, J. Hone, J. Shan, T. F. Heinz, *Phys. Rev. Lett.* **105**, 136805 (2010).
- [9] S. Cahangirov, M. Topsakal, E. Akturk, H. Sahin, S. Ciraci, *Phys. Rev. Lett.* **102**, 236804 (2009).
- [10] H. Sahin, S. Cahangirov, M. Topsakal, E. Bekaroglu, E. Akturk, R. T. Senger, S. Ciraci, *Phys. Rev. B* **80**, 155453 (2009).
- [11] K. Omri, A. Bettaibi, K. Khirouni, L. El Mir, *Physica B: Condens. Matter.* **537**, 167 (2018).
- [12] K. Omri, I. Najeh, L. El Mir, *Ceram. Int.* **42**, 8940 (2016).
- [13] M. Kaddes, K. Omri, N. Kouaydi, M Zemzemi, *Appl. Phys. A* **124**, 518 (2018).
- [14] Ü. Özgür, Y. I. Alivov, C. Liu, A. Teke, M. A. Reshchikov, S. Dogan, V. Avrutin, S. J. Cho, H. J. Morkoç, *Appl. Phys. Rev.* **98**, 041301 (2005).
- [15] W. Shan, B. D. Little, A. J. Fischer, J. J. Song, B. Goldenberg, W. G. Perry, M. D. Bremser, R. F. Davis, *Phys. Rev. B* **54**, 16369 (1997).
- [16] D. C. Look, *Mat. Sc. Eng. B* **80**, 383 (2001).
- [17] H. Kim, J. S. Horowitz, S. B. Quadri, D. B. Chrisey,

- Thin Solid Films **420**, 107 (2002).
- [18] R. L. Hoffman, B. J. Norris, J. F. Wager, *Appl. Phys. Lett.* **82**, 733 (2003).
- [19] A. P. Chatterjee, P. M. Mitra, A. K. Mukhopadhyay, *J. Mater. Sci.* **34**, 4225 (1999).
- [20] T. Minami, T. Miyata, K. Ihara, Y. Minamino, S. Tsukada, *Thin Solid Films* **494**, 47 (2006).
- [21] W. J. Jeong, S. K. Kim, G. C. Park, *Thin Solid Films* **506**, 180 (2006).
- [22] C. L. Freeman, F. Claeysens, N. L. Allan, J. H. Harding, *Phys. Rev. Lett.* **96**, 066102 (2006).
- [23] Z. C. Tu, X. Hu, *Phys. Rev. B* **74**, 035434 (2006).
- [24] C. Tusche, H. L. Meyerheim, J. Kirschner, *Phys. Rev. Lett.* **99**, 026102 (2007).
- [25] A. J. Kulkarni, M. Zhou, K. Sarasamak, S. Limpijumngong, *Phys. Rev. Lett.* **97**, 105502 (2006).
- [26] F. Claeysens, C. L. Freeman, N. L. Allan, Y. Sun, M. N. R. Ashfold, J. H. Harding, *J. Mater. Chem.* **15**, 139 (2005).
- [27] L. Zhang, H. Huang, *Appl. Phys. Lett.*, **89**, 183111 (2006).
- [28] L. Zhang, H. Huang, *Appl. Phys. Lett.* **90**, 023115 (2007).
- [29] D. Wu, M. G. Lagally, F. Liu, *Phys. Rev. Lett.* **107**, 236101 (2011).
- [30] P. Hohenberg, W. Kohn, *Phys. Rev.* **136**, 864 (1964).
- [31] X. Gonze, B. Amadon, P.-M. Anglade, J.-M. Beuken, F. Bottin, P. Boulanger, F. Bruneval, D. Caliste, R. Caracas, M. Côté, T. Deutsch, L. Genovese, Ph. Ghosez, M. Giantomassi, S. Goedecker, D. R. Hamann, P. Hermet, F. Jollet, G. Jomard, S. Leroux, M. Mancini, S. Mazevet, M. J. T. Oliveira, G. Onida, Y. Pouillon, T. Rangerl, G.-M. Rigmanese, D. Sangalli, R. Shaltaf, M. Torrent, M. J. Verstraete, G. Zerah, J. W. Zwanziger *Comput. Phys. Commun.* **180**, 2582 (2009).
- [32] N. Troullier, J. L. Martins, *Phys. Rev. B* **43**(3), 1993 (1991).
- [33] M. Fuchs, M. Scheffler, *Comput. Phys. Commun.* **119**, 67 (1999).
- [34] J. P. Perdew, Y. Wang, *Phys. Rev. B* **45**, 13244 (1992).
- [35] D. M. Ceperley, B. J. Alder, *Phys. Rev. Lett.* **45**, 566 (1980).
- [36] J. Perdew, K. Burke, M. Ernzerhof, *Phys. Rev. Lett.* **77**, 3865 (1996).
- [37] H. J. Monkhorst, J. D. Pack, *Phys. Rev. B* **13**, 5188 (1976).
- [38] A. Kokalj, *Comput. Mater. Sci.* **28**, 155 (2003).
- [39] A. A. Ashrafi, A. Ueta, H. Kumano, I. Suemune, *J. Cryst. Growth* **221**, 435 (2000).
- [39] R. G. Parr, W. Yang, *Density functional theory of atoms and molecules*, Oxford university Press, New York 1989.
- [40] F. D. Murnaghan, *Proc. Natl. Acad. Sci., USA* **30**, 244 (1944).
- [42] S. Desgreniers, *Phys. Rev. B* **58**, 14102 (1998).
- [43] M. Zemzemi, S. Alaya, *Mat. Sci. Appl.* **6**, 661 (2015).
- [44] M. P. Molepo, D. P. Joubert, *Phys. Rev. B* **84**, 094110 (2011).
- [45] H. Liu, J. S. Tse, H. K. Mao, *J. Appl. Phys.* **100**, 093509 (2006).
- [46] F. G. Kuang, X. Y. Kuang, S. Y. Kang, M. M. Zhong, X. W. Sun, *Mater. Sci. Semicond. Process.* **31**, 700 (2015).
- [47] J. Kang, Y. Zhang, Y. H. Wen, J. C. Zheng, Z. Z. Zhu, *Phys. Lett. A* **374**, 1054 (2010).
- [48] Q. B. Wang, C. Zhou, J. Wu, T. Lü, K. H. He, *Comput. Mater. Sci.* **102**, 196 (2015).
- [49] D. E. Sands, *Introduction to Crystallography*. Benjamin Cummings, Reading, MA, U. S. A. (1969).
- [50] J. C. Charlier, X. Gonze, J. P. Michenaud, *Phys. Rev. B* **43**, 4579 (1991).
- [51] R. Tatar, S. Rabii, *Phys. Rev. B* **25**, 4126 (1982).
- [52] W. Hu, Z. Li, J. Yang, *J. Chem. Phys.* **138**, 124706 (2013).
- [53] J. Lei, M. C. Xu, S. J. Hu, *J. Appl. Phys.* **118**, 104302 (2015).
- [54] S. Reich, J. Maultzsch, C. Thomsen, *Phys. Rev. B* **66**, 035412 (2002).
- [55] G. Mukhopadhyay, H. Behera, [arXiv: 1210.3308].
- [56] A. T. N'Diaye, J. Coraux, T. N. Plasa, C. Busse, T. Michely, *New J. Phys.* **10**, 043033 (2008).
- [57] M. Topsakal, S. Cahangirov, E. Bekaroglu, S. Ciraci, *Phys. Rev. B* **80**, 235119 (2009).
- [58] B. Amrani, I. Chiboub, S. Hiadsi, T. Benmessabih, N. Hamdadou, *Solid State Commun.* **137**, 395 (2006).
- [59] Y. L. Su, Q. Y. Zhang, C. Y. Pu, X. Tang, J. J. Zhao, *Solid State Commun.* **223**, 19 (2015).
- [60] Y. J. Zeng, K. Schouteden, M. N. Amini, S. C. Ruan, Y. F. Lu, Z. Z. Ye, B. Partoens, D. Lamoen, C. V. Haesendonck, *ACS Appl. Mater. Interfaces* **7**, 10617 (2015).
- [61] Z. G. Yu, H. Gong, P. J. Wu, *Cryst. Growth* **287**, 199 (2006).
- [62] R. John, S. Padmavathi, *Cryst. Struct. Theory Appl.* **5**, 24 (2016).
- [63] W. Hume-Rothery, *The Metallic State*, Oxford University Press, New York, 1931.
- [64] Z. C. Tu, *J. Comput. Theor. Nanosci.* **7**, 1182 (2010).
- [65] Y. Wang, Y. Ding, J. Ni, S. Shi, C. Li, J. Shi, *Appl. Phys. Lett.* **96**, 213117 (2010).
- [66] S. Lany, A. Zunger, *Phys. Rev. B* **78**, 235104 (2008).
- [67] A. H. Castro, N. K. Novoselov, *Rep. Prog. Phys.* **74**, 082501 (2011).

*Corresponding author: mzemzemi@gmail.com